Filomat 39:30 (2025), 10799–10822
https://doi.org/10.2298/FIL2530799B

Published by Faculty of Sciences and Mathematics,
University of Niš, Serbia
Available at: http://www.pmf.ni.ac.rs/filomat

Identification of the initial value in a space-time fractional diffusion equation

Mohamed BenSalah[a], Salih Tatar[b,*]

[a]*Department of Computer Science, ISSAT of Sousse, University of Sousse, Tahar Ben Achour Street, Sousse 4003, Tunisia*
[b]*Department of Mathematics & Computer Science, College of Science and General Studies, Alfaisal University, Riyadh, Saudi Arabia*

Abstract. This study addresses an inverse problem of identifying the initial condition in a space-time fractional diffusion equation, where both the time derivative and the spatial operator are of fractional order. Specifically, the goal is to reconstruct the unknown initial state from measurements of the system at a fixed final time. We first establish the well-posedness of the associated direct problem and prove the uniqueness of the inverse problem's solution using eigenfunction expansions. However, we also demonstrate that the inverse problem is severely ill-posed, as small perturbations in the data can lead to large deviations in the solution. To obtain stable reconstructions, we reformulate the inverse problem as a Tikhonov-regularized optimization problem that balances data fidelity with solution smoothness. The resulting variational problem is solved numerically using a conjugate gradient method enhanced by Morozov's discrepancy principle for adaptive stopping. The performance and stability of the proposed approach are validated through several numerical experiments involving both smooth and discontinuous initial conditions. Our results show that the method provides accurate reconstructions even in the presence of moderate to high levels of noise, confirming its effectiveness and robustness for practical applications in anomalous diffusion modeling.

Nomenclature

α :	Fractional order of the time derivative	Δx :	Space step
α_k :	Conjugate coefficient in the kth iteration	Γ :	Gamma function
$\chi_{(-1,1)}$:	Characteristic function of the interval $(-1,1)$	$\|\|.\|\|_{H^s(\Omega)}$:	H^s norm in Ω
δ :	Dirac delta function	$\|.\|_{H^s(\Omega)}$:	Aronszajn-Slobodeckij seminorm
Δt :	Time step	$\|\|.\|\|_{L^2(\Omega)}$:	L^2 norm in Ω

2020 *Mathematics Subject Classification*. Primary 35R30; Secondary 35R11, 47A52, 49N30, 34K28.
Keywords. Fractional Laplacian, Inverse problem, Fractional diffusion equation, Existence and uniqueness, Ill-posedness, Regularization method; Optimization problem.
Received: 19 December 2023; Revised: 17 July 2025; Accepted: 28 September 2025
Communicated by Marko Petković
* Corresponding author: Salih Tatar
Email addresses: mohamed.bensalah@fsm.rnu.tn (Mohamed BenSalah), statar@alfaisal.edu (Salih Tatar)
ORCID iDs: https://orcid.org/0000-0002-7301-250X (Mohamed BenSalah), https://orcid.org/0000-0003-4669-0169 (Salih Tatar)

$\mathcal{B}_s$: Bilinear form associated to the space $\widetilde{H}^s(\Omega)$

$\mathcal{I}_s$: Stopping index

$\mathcal{R}_k$: Residual in the kth iteration

$\mathcal{T}_v$: Objective function

μ : Relative noise level

Ω : Domain of $\mathbb{R}^d$, $d \geq 1$

Ω^c : Complement of Ω in $\mathbb{R}^d$

$\overline{\Omega}$: Closure of Ω

θ : Noise level

$\widetilde{H}^s(\Omega)$: Set of functions in $H^s\left(\mathbb{R}^d\right)$ supported within $\overline{\Omega}$

ζ_k : Step size in the kth iteration

$C_{d,s}$: Normalization constant

d_k : Descent direction in the kth iteration

E_k : L^2 error in the kth iteration

$E_{\alpha,\beta}$: Mittag-Leffler function

h : Measured data

$H^\alpha(0,T)$: Fractional Sobolev space in time

$H^s(\mathbb{R}^d)$: Fractional Sobolev space on $\mathbb{R}^d$

$H^s(\Omega)$: Fractional Sobolev space on Ω

$L^2(\Omega)$: Set of square integrable functions on Ω

s : Fractional order of the space derivative

T : Final time

P.V : Principal value

rand(.) : Random function

1. Introduction

Let $T > 0$, $\Omega \subset \mathbb{R}^d$ and $d \geq 1$ be an open, bounded domain. We consider the following initial-boundary value problem for a space-time fractional diffusion equation with homogeneous Dirichlet boundary and initial conditions:

$$\begin{cases} \partial_t^\alpha u(x,t) = -(-\Delta)^s u(x,t), & (x,t) \in \Omega \times (0,T), \\ u(x,t) = 0, & (x,t) \in \Omega^c \times (0,T), \\ u(x,0) = g(x), & x \in \Omega, \end{cases} \tag{1}$$

where Ω^c is the complement of Ω in $\mathbb{R}^d$, $g(x) \in L^2(\Omega)$ is an initial function, ∂_t^α denotes the left Caputo fractional derivative of order $0 < \alpha < 1$ (see, e.g., [31]), defined by

$$\partial_t^\alpha v(t) := \frac{1}{\Gamma(1-\alpha)} \int_0^t \frac{v'(\tau)}{(t-\tau)^\alpha} \mathrm{d}\tau, \tag{2}$$

and $(-\Delta)^s$ is the non-local fractional Laplacian operator of order $s \in (0,\, 1)$, defined by

$$(-\Delta)^s u(x) = C_{d,s}\ \text{P.V.} \int_{\mathbb{R}^d} \frac{u(x) - u(y)}{|x-y|^{d+2s}} dy. \tag{3}$$

In (2) and (3), $\Gamma(.)$ is the Gamma function, $C_{d,s}$ is a normalization constant, defined by

$$C_{d,s} = \frac{2^{2s} s \Gamma\left(s + \frac{d}{2}\right)}{\pi^{d/2} \Gamma(1-s)},$$

and "P.V." is the principal value of the integral, defined by

$$\text{P.V.} \int_{\mathbb{R}^d} \frac{v(x) - v(y)}{|x-y|^{d+2s}} dy = \lim_{\varepsilon \downarrow 0} \int_{\{y \in \mathbb{R}^d, |y-x| > \varepsilon\}} \frac{v(x) - v(y)}{|x-y|^{d+2s}} dy.$$

Remark 1.1. *The fractional Laplace operator is also defined by either Spectral/Fourier definition, or standard Laplacian, or Lévy process, or directional representation. In this work, we use the fractional Laplace operator by singular integral definition as in* (3)*. We refer the readers to [14] and [37] for more details regarding the Fractional Laplacian operator.*

For given $(\alpha, s) \in (0,1)^2$, and $g(x) \in L^2(\Omega)$, the problem (1) is called the direct(forward) problem. Like most direct problems of mathematical physics, the problem (1) is well-posed, see for example, [49] and [11]. The inverse problem here consists of determining the function $g(x)$, by means of the observation data (additional data) $u(x,T) = h(x)$, $x \in \Omega$.

The space-time fractional diffusion equation $\partial_t^\alpha u = -(-\Delta)^s u$ with $0 < \alpha, s < 1$ is used to model anomalous diffusion [40]. Here, the fractional derivative in time is used to describe particle sticking and trapping phenomena, while the fractional space derivative is used to model long particle jumps. These two effects combined together produce a concentration profile with a sharper peak and heavier tails. In the fractional diffusion equations, the fractional time derivative with $0 < \alpha < 1$ is used to model slow diffusion, and the exponent s is related to the parameter specifying the large-time behavior of the waiting-time distribution function and particular cases of the infinitesimal generators of Lévy stable diffusion processes and appear in anomalous diffusions in plasmas, flame propagation and chemical reactions in liquids, population dynamics, geophysical fluid dynamics, see [44], [30], [14] and some of the references cited therein. Recently, there has been a growing interest in inverse problems with fractional derivatives. These problems are physically and practically very important. For example in [12], the authors prove a uniqueness result for a one-dimensional time-fractional diffusion equation. The proof is based on the eigenfunction expansion of the weak solution to the initial value/boundary value problem and the Gel'fand–Levitan theory. In [28], they study an inverse problem of recovering a spatially varying potential term in a one-dimensional time-fractional diffusion equation from the flux measurements taken at a single fixed time corresponding to a given set of input sources. The unique identifiability of the potential is shown for two cases, i.e. the flux at one end and the net flux, provided that the set of input sources forms a complete basis in $L^2(0,1)$. An algorithm of the Quasi-Newton type is proposed for the efficient and accurate reconstruction of the coefficient from finite data, and the injectivity of the Jacobian is discussed. In [38], the authors consider a backward problem in time for a time-fractional partial differential equation in the one-dimensional case, which describes the diffusion process in porous media related to the continuous time random walk problem. The backward problem is ill-posed and they propose a regularizing scheme by the quasi-reversibility with fully theoretical analysis and test its numerical performance. With the help of the memory effect of the fractional derivative, it is found that the property of the initial status of the medium can be recovered in an efficient way. In [46], for a time-fractional diffusion equation with source term, they discuss an inverse problem of determining a spatially varying function of the source by final overdetermining data. They prove that this inverse problem is well-posed in the Hadamard's sense except for a discrete set of values of diffusion constants. In [47], the authors consider initial value/boundary value problems for a fractional diffusion-wave equation. For $\alpha \in (0,1)$, they prove stability in the backward problem in time, the uniqueness in determining an initial value, the uniqueness of solution by the decay rate as $t \to \infty$ and stability in an inverse source problem of determining t - dependent factor in the source by observation at one point over $(0,T)$. The authors study an inverse source problem for a fractional diffusion equation in [54]. Under the assumption that the unknown source term is time-independent, an analytical solution can be deduced based on the method of the eigenfunction expansion. Then, the uniqueness of the inverse problem is proved by analytic continuation and the Laplace transform. The paper [34] deals with an inverse problem of simultaneously identifying the space-dependent diffusion coefficient and the fractional order in the one dimensional time-fractional diffusion equation with smooth initial functions by using boundary measurements. The uniqueness results for the inverse problem are proved on the basis of the inverse eigenvalue problem, and the Lipschitz continuity of the solution operator is established. In [18], the authors study an inverse random source problem for the time-fractional diffusion equation, where the source is driven by a fractional Brownian motion. Given the random source, the direct problem is to study the stochastic time-fractional diffusion equation. The inverse problem is to determine the statistical properties of the

source from the expectation and variance of the final time data. For the direct problem, the authors show that it is well-posed and has a unique mild solution under a certain conditions. For the inverse problem, the uniqueness is proved and the instability is characterized. The authors consider an inverse boundary value problem for diffusion equations with multiple fractional time derivatives and they prove the uniqueness in determining the number of fractional time-derivative terms, the orders of the derivatives and spatially varying coefficients in [35]. However, there are only a few papers involving both fractional Laplacian and fractional time derivatives. For instance, in [49], the authors study a nonlocal inverse problem related to the space-time fractional equation. The existence of the solution for the inverse problem is proved by using the quasi-solution method which is based on minimizing an error functional between the output data and the additional data. In this context, an input-output mapping is defined and continuity of the mapping is established. The uniqueness of the solution for the inverse problem is also proved by using eigenfunction expansion of the solution and some basic properties of fractional Laplacian. A numerical method based on discretization of the minimization problem, steepest descent method, and least squares approach is proposed for the solution of the inverse problem. A nonlocal inverse source problem for a one-dimensional space-time fractional diffusion equation is studied in [50]. At first, they define and analyze the direct problem for the space-time fractional diffusion equation. Later, they define the inverse source problem. Furthermore, they set up an operator equation and derive the relation between the solutions of the operator equation and the inverse source problem. They also prove some important properties of the operator. By using these properties and the analytic Fredholm theorem, it is proved that the inverse source problem is well posed, i.e. the solution can be determined uniquely and depends continuously on additional data. In [23], they consider a nonlocal inverse problem and show that the fractional exponents β, α and γ, where β is the order of the time-fractional derivative and α and γ are exponents of fractional Laplacian operator, are determined uniquely by the data $u(x,T) = h(x)$, $0 \leq t \leq T$. The existence of the solution for the inverse problem is proved using the quasi-solution method which is based on minimizing an error functional between the output data and the additional data. In this context, an input-output mapping is defined and its continuity is established. The uniqueness of the solution for the inverse problem is proved by means of eigenfunction expansion of the solution to the forward problem and some basic properties of fractional Laplacian. In [43], the authors study a diffusion equation of the Kirchhoff type with a conformable fractional derivative. The global existence and uniqueness of mild solutions are established. Some regularity results for the mild solution are also derived. This study can be regarded as a continuation of the series of works mentioned above on fractional inverse problems.

This paper is organized as follows: In section 2, we present some preliminaries used throughout the paper. In section 3, we formulate the direct and inverse problems, we prove that the considered inverse problem has a unique solution and the inverse problem is ill-posed, we also reformulate the inverse problem as a minimization problem. Section 4 is concerned with the proposed reconstruction approach. Some numerical simulations are presented in Section 5. The conclusions and possible directions on the problem are given in Section 6.

2. Preliminaries

In this section, we set some basic notations and recall some definitions and theorems.

By $L^2(\Omega)$, we denote the usual L^2-space with the inner product $(\,,\,)$ and by $H_0^1(\Omega)$, $H^1(\Omega)$, etc we denote the usual Sobolev spaces. By $H^\alpha(0,T)$, we denote the fractional Sobolev space in time (see Adams [5]). Especially, for $s \in (0,1)$, the fractional Sobolev space $H^s(\Omega)$ is defined by

$$H^s(\Omega) = \left\{ u \in L^2(\Omega) : |u|_{H^s(\Omega)} := \left(\iint_{\Omega^2} \frac{|u(x)-u(y)|^2}{|x-y|^{d+2s}} dxdy \right)^{\frac{1}{2}} < \infty \right\}.$$

Its natural norm is defined by

$$\|u\|_{H^s(\Omega)} := \left(\|u\|^2_{L^2(\Omega)} + |u|^2_{H^s(\Omega)} \right)^{1/2}.$$

Moreover, we define the fractional space $\tilde{H}^s(\Omega)$ of order $s \in (0,1)$ as follows:

$$\widetilde{H}^s(\Omega) := \left\{ u \in H^s\left(\mathbb{R}^d\right) : \operatorname{supp} u \subset \overline{\Omega} \right\}.$$

It may also be defined through interpolation as follows:

$$\widetilde{H}^s(\Omega) := \left[L^2(\Omega), H_0^1(\Omega) \right]_s.$$

The bilinear form associated to the space $\widetilde{H}^s(\Omega)$ is given by

$$\mathcal{B}_s(u,v) := C_{d,s} \iint_{(\mathbb{R}^d\times\mathbb{R}^d)\setminus(\Omega^c\times\Omega^c)} \frac{(u(x)-u(y))(v(x)-v(y))}{|x-y|^{d+2s}} dx\, dy.$$

Proposition 2.1 (see [15, 16]). *Let $u, v : \mathbb{R}^d \longrightarrow \mathbb{R}$ be smooth functions, then*

$$\int_\Omega v(x)(-\Delta)^s u(x) dx = \frac{\mathcal{B}_s(u,v)}{2} - \int_{\Omega^c} v(x)\mathcal{N}_s u(x) dx,$$

where $\mathcal{N}_s$ denotes the non-local Neumann operator associated to $(-\Delta)^s$ and defined as

$$\mathcal{N}_s v(x) := C_{d,s} \int_\Omega \frac{v(x)-v(y)}{|x-y|^{d+2s}} dy.$$

The following proposition is concerned with a fractional integration by parts formula. It gives the relationship between Caputo and Riemann-Liouville fractional derivatives.

Proposition 2.2 (see [6, 7]). *Let $\alpha \in (0,1)$. Let μ_1 and μ_2 be two absolutely integrable functions. Then, we have*

$$\int_0^T \mu_2(t)\partial_t^\alpha \mu_1(t) dt = \int_0^T \mu_1(t) D_t^\alpha \mu_2(t) dt + \left[\mu_1(t) J_{T^-}^{1-\alpha}\mu_2(t)\right]_{t=0}^{t=T},$$

where $J_{T^-}^{1-\alpha}\mu_2(t)$ denotes the right Riemann-Liouville fractional integral of $\mu_2(t)$ defined by

$$J_{T^-}^{1-\alpha}\mu_2(t) = \frac{1}{\Gamma(1-\alpha)} \int_t^T \frac{\mu_2(\tau)}{(\tau-t)^\alpha} \mathrm{d}\tau,$$

and $D_t^\alpha \mu_2(t)$ denotes the backward Riemann-Liouville fractional derivative defined by

$$D_t^\alpha \mu_2(t) := -\left(J_{T^-}^{1-\alpha}\mu_2(t)\right)' = \frac{-1}{\Gamma(1-\alpha)} \frac{d}{dt} \int_t^T \frac{\mu_2'(\tau)}{(\tau-t)^\alpha} \mathrm{d}\tau.$$

Let us introduce the Mittag-Leffler function which is defined on the complex set $\mathbb{C}$ by

$$E_{\alpha,\beta}(z) := \sum_{k=0}^{\infty} \frac{z^k}{\Gamma(\alpha k+\beta)}, \quad z \in \mathbb{C},$$

where $\alpha > 0$ and $\beta \in \mathbb{R}$ are arbitrary constants. Notice that this complex function depends on two parameters. In particular, it generalizes the exponentials in view of the identity $E_{1,1}(z) = e^z$ for all $z \in \mathbb{C}$. Moreover, it plays a central role in fractional diffusion equations. The following results of this family of functions are useful to derive the solution representation of the direct problem (1).

Lemma 2.3. *[13, Theorem 4.3] Let $\alpha > 0$ and $\lambda > 0$, then we have*

$$\partial_t^\alpha E_{\alpha,1}\left(-\lambda t^\alpha\right) = -\lambda E_{\alpha,1}\left(-\lambda t^\alpha\right), \quad t > 0.$$

Moreover, the following identity holds for integer-order differentiation:

$$\frac{d}{dt} E_{\alpha,1}\left(-\lambda t^\alpha\right) = -\lambda\, t^{\alpha-1} E_{\alpha,\alpha}\left(-\lambda t^\alpha\right), \quad t > 0.$$

Lemma 2.4. *[44, Theorem 1.6] Let $0 < \alpha < 1$ and $\pi\alpha/2 < \mu < \pi\alpha$. Then there exists a constant $C_0 = C_0(\alpha,\mu) > 0$ such that*

$$\left|E_{\alpha,1}(z)\right| \leqslant \frac{C_0}{1+|z|}, \quad \mu \leqslant |\arg(z)| \leqslant \pi.$$

3. The direct and the inverse problems

In this section, we formulate the direct and inverse problems, then we prove that the considered inverse problem has a unique solution. We also prove that the inverse problem is ill-posed. First of all, we need to define a solution formula for the direct problem (1). By using the eigenfunction expansion method, following [4], [11], [39], [47], we get the following useful formula for the weak solution of the direct problem (1):

$$u(x,t) := \sum_{k=1}^{\infty} g_k \, E_{\alpha,1}\left(-\lambda_k t^{\alpha}\right) \varphi_k(x), \quad \forall (x,t) \in \Omega \times (0,T), \tag{4}$$

where $g_k = (g, \varphi_k)$ and the family $\{(\varphi_k, \lambda_k)\}_{k\geq 1}$ represents the eigenpairs of the fractional Laplace operator $(-\Delta)^s$ on Ω with homogeneous Dirichlet condition, i.e.

$$\begin{cases} (-\Delta)^s \varphi_k = \lambda_k \varphi_k & \text{in } \Omega, \\ \varphi_k = 0 & \text{in } \Omega^c. \end{cases}$$

In addition, it is well-known that the fractional Laplacian operator has a sequence of eigenvalues satisfying

$$0 < \lambda_1 \leq \lambda_2 \leq \cdots \leq \lambda_k \leq \cdots \text{ and } \lim_{k\to+\infty} \lambda_k = +\infty.$$

Besides, the set of eigenfunctions $\{\varphi_k\}_{k=1}^{\infty}$ forms an orthonormal basis of $L^2(\Omega)$.

Remark 3.1. *Unlike the classical Laplacian, it is proved in [22, 45] that eigenfunctions of the fractional Laplacian are in general non-smooth. More precisely, for each k, $k = 1, 2, 3, \cdots$, the eigenfunction φ_k belongs to $H^{s+1/2-\epsilon}\left(\mathbb{R}^d\right)$ where $\epsilon > 0$ is an arbitrary small real number.*

Following the same idea given in [4, 47] and based on the formula (4) and Lemmas 2.3 and 2.4, we have the following theorem that states the regularity result for the solution of the problem (1):

Theorem 3.2. *Let $(\alpha, s) \in (0,1)^2$, and $g \in L^2(\Omega)$ be given. Then, problem* (1) *admits a unique weak solution $u \in \mathcal{H}^{\alpha,s}(0,T;\Omega)$. Furthermore, there exists a constant $C > 0$ such that*

$$\left\|\partial_t^{\alpha} u\right\|_{C([0,T];L^2(\Omega))} \leq C \|g\|_{L^2(\Omega)},$$

and

$$\left\|\partial_t^{\alpha} u(.,t)\right\|_{L^2(\Omega)} + \|u(.,t)\|_{H^{s+\gamma}(\Omega)} \leq C\, t^{-\alpha} \|g\|_{L^2(\Omega)},$$

where

$$\mathcal{H}^{\alpha,s}(0,T;\Omega) := \left\{ v \in C([0,T];L^2(\Omega)) \cap C((0,T];\widetilde{H}^s(\Omega) \cap H^{s+\gamma}(\Omega)) \text{ such that } \partial_t^{\alpha} v \in C((0,T];L^2(\Omega)) \right\},$$

$\gamma := \min\{s, 1/2 - \varepsilon\}$ and $\varepsilon > 0$ arbitrarily small.

The inverse problem that we consider consists of identifying the initial value g, from noise measurement of the final time solution. More precisely, the considered inverse problem can be formulated as finding $g^{\star} \in L^2(\Omega)$ and $u^{\star} \in \mathcal{H}^{\alpha,s}(0,T;\Omega)$ in the following problem:

$$\begin{cases} \partial_t^{\alpha} u^{\star}(x,t) = -(-\Delta)^s u^{\star}(x,t), & (x,t) \in \Omega \times (0,T), \\ u^{\star}(x,t) = 0, & (x,t) \in \Omega^c \times (0,T), \\ u^{\star}(x,0) = g^{\star}(x), & x \in \Omega, \\ u^{\star}(x,T) = h(x), & x \in \Omega. \end{cases} \tag{5}$$

The following proposition is concerned with the series representation of the solution of problem (5) using the eigenfunction expansion method.

Proposition 3.3. *Let $h \in L^2(\Omega)$ be a given function. Then, the solution of the problem* (5) *can be represented as follows*

$$g^\star(x) = \sum_{k=1}^{\infty} \frac{\left(h, \varphi_k\right)}{E_{\alpha,1}(-\lambda_k T^\alpha)} \varphi_k(x),$$

and

$$u^\star(x,t) = \sum_{k=1}^{\infty} \frac{\left(h, \varphi_k\right)}{E_{\alpha,1}(-\lambda_k T^\alpha)} E_{\alpha,1}(-\lambda_k t^\alpha) \varphi_k(x).$$

Proof. From (4), the solution of

$$\begin{cases} \partial_t^\alpha u^\star(x,t) = -(-\Delta)^s u^\star(x,t), & (x,t) \in \Omega \times (0,T), \\ u^\star(x,t) = 0, & (x,t) \in \Omega^c \times (0,T), \\ u^\star(x,0) = g^\star(x), & x \in \Omega, \end{cases}$$

is given by

$$u^\star(x,t) := \sum_{k=1}^{\infty} (g^\star, \varphi_k)\, E_{\alpha,1}\left(-\lambda_k t^\alpha\right)\, \varphi_k(x). \tag{6}$$

By taking $t = T$ and using the fact that $u^\star(., T) = h$ in Ω, we get

$$h = \sum_{k=1}^{\infty} (g^\star, \varphi_k)\, E_{\alpha,1}\left(-\lambda_k T^\alpha\right)\, \varphi_k(x).$$

Multiplying both sides of the above equation by φ_k and integrating with respect to x, we get

$$\left(h, \varphi_k\right) = \left(g^\star, \varphi_k\right) E_{\alpha,1}(-\lambda_k T^\alpha).$$

Since $E_{\alpha,1}(-\lambda_k T^\alpha) > 0$, it follows:

$$\left(g^\star, \varphi_k\right) = \frac{\left(h, \varphi_k\right)}{E_{\alpha,1}(-\lambda_k T^\alpha)}. \tag{7}$$

Hence $g^\star$ is given by

$$g^\star(x) = \sum_{k=1}^{\infty} \frac{\left(h, \varphi_k\right)}{E_{\alpha,1}(-\lambda_k T^\alpha)} \varphi_k(x).$$

Substituting (7) into (6) yields

$$u^\star(x,t) = \sum_{k=1}^{\infty} \frac{\left(h, \varphi_k\right)}{E_{\alpha,1}(-\lambda_k T^\alpha)} E_{\alpha,1}(-\lambda_k t^\alpha) \varphi_k(x).$$

The proof is complete. □

Now we prove a uniqueness theorem. Let u_1 and u_2 be the solutions of the problem (1) correspond to the initial values $g_j \in L^2(\Omega)$, $j = 1, 2$, respectively.

Theorem 3.4. *Let u_1 and u_2 be the solutions of the problem* (1). *If $u_1(x,T) = u_2(x,T)$, $x \in \Omega$, then we have*

$$g_1 = g_2 \text{ in } \Omega.$$

Proof. Using the series representations of solutions u_1 and u_2, we have

$$u_j(x,T) = \sum_{k=1}^{\infty} \left\{ \left(g_j, \varphi_k\right) E_{\alpha,1}\left(-\lambda_k T^{\alpha}\right) \right\} \varphi_k(x), \quad \text{for } j = 1,2. \tag{8}$$

As $u_1(.,T) = u_2(.,T)$ in Ω, we deduce that

$$\sum_{k=1}^{\infty} \left\{ \left(g_1, \varphi_k\right) E_{\alpha,1}\left(-\lambda_k T^{\alpha}\right) \right\} \varphi_k(x) = \sum_{k=1}^{\infty} \left\{ \left(g_2, \varphi_k\right) E_{\alpha,1}\left(-\lambda_k T^{\alpha}\right) \right\} \varphi_k(x).$$

First, we multiply both sides of the above equality by $\varphi_k(x)$ and integrate the resulting equation with respect to x. Then by using the fact that $\varphi_k = 0$ in Ω^c, we obtain

$$\left(g_1, \varphi_k\right) E_{\alpha,1}\left(-\lambda_k T^{\alpha}\right) = \left(g_2, \varphi_k\right) E_{\alpha,1}\left(-\lambda_k T^{\alpha}\right), \text{ for all } k \geq 1.$$

It follows:

$$\left(g_1 - g_2, \varphi_k\right) E_{\alpha,1}\left(-\lambda_k T^{\alpha}\right) = 0, \text{ for all } k \geq 1.$$

Since $E_{\alpha,1}\left(-\lambda_k t^{\alpha}\right) > 0$, $t > 0$ is completely monotonic (see [21]), $E_{\alpha,1}\left(-\lambda_k T^{\alpha}\right) > 0$, we have the following:

$$\left(g_1, \varphi_k\right) = \left(g_2, \varphi_k\right), \text{ for all } k \geq 1,$$

implies $g_1 = g_2$ in Ω. Thus, the proof is complete. □

To find an estimate of g from the additional data h, the most common method is to minimize the discrepancy

$$\left\| \mathcal{A}(g) - h \right\|^2_{L^2(\Omega)},$$

where the operator $\mathcal{A}$ is defined by

$$\begin{aligned} \mathcal{A} : L^2(\Omega) &\longrightarrow L^2(\Omega), \\ g &\longmapsto u(.,T). \end{aligned} \tag{9}$$

We know that the linear operator $\mathcal{A}$ is self-adjoint, for more details we refer the readers to [29, 51]. Next, we prove that the operator $\mathcal{A}$ is compact.

Proposition 3.5. *The linear operator $\mathcal{A}$ defined by* (9) *is a compact operator from $L^2(\Omega)$ into $L^2(\Omega)$.*

Proof. By (4) and (9), we deduce that

$$\mathcal{A}(g) = \sum_{k=1}^{+\infty} g_k \, E_{\alpha,1}\left(-\lambda_k T^{\alpha}\right) \, \varphi_k(x), \ \forall g \in L^2(\Omega). \tag{10}$$

We define the finite rank operators $\mathcal{A}_N$ as follows:

$$\mathcal{A}_N(g) := \sum_{k=1}^{N} g_k \, E_{\alpha,1}\left(-\lambda_k T^{\alpha}\right) \, \varphi_k(x), \ \forall g \in L^2(\Omega). \tag{11}$$

From (10) and (11), we get

$$\|\mathcal{A}(g) - \mathcal{A}_N(g)\|^2_{L^2(\Omega)} = \sum_{k=N+1}^{+\infty} \left| E_{\alpha,1}\left(-\lambda_k T^{\alpha}\right) \right|^2 |g_k|^2.$$

Thanks to Lemma 2.4, we obtain

$$\|\mathcal{A}(g) - \mathcal{A}_N(g)\|_{L^2(\Omega)} \leqslant \frac{C_0}{T^\alpha \lambda_N} \|g\|_{L^2(\Omega)}.$$

Therefore, $\|\mathcal{A}(g) - \mathcal{A}_N(g)\|_{L^2(\Omega)} \longrightarrow 0$ in the sense of operator norm in $L(L^2(\Omega); L^2(\Omega))$ as $N \longrightarrow \infty$. □

Since equations with compact operators are ill-posed, the inverse problem under consideration is also ill-posed.

It is well known that in practical applications, the given data h is typically not exact, but rather a distortion of the unknown $u[g_{exact}]$. This distortion is often modeled by an additive noise or an error term θ. Denote by h^θ a noisy function of h satisfying

$$\|h - h^\theta\| \leqslant \theta.$$

Due to this noise associated with the measured data, the solution becomes very sensitive to the measured data, which causes severe numerical instabilities. Thus, the considered inverse problem is ill-posed in the sense of Hadamard [24]. In the following, we consider an example to see that the considered inverse problem is ill-posed. More precisely, we will prove that the solution to the inverse problem does not depend continuously on the final time data h. In doing so, let us choose an input final data h_1 as

$$h_p(x) = \frac{\varphi_p(x)}{\sqrt{\lambda_p}}.$$

From Proposition 3.3, the initial data corresponding to h^p is represented as follows:

$$g^p(x) = \sum_{k=1}^{\infty} \frac{\left(h_1, \varphi_k\right)}{E_{\alpha,1}(-\lambda_k T^\alpha)} \varphi_k(x).$$

Using the fact the set of eigenfunctions $\{\varphi_k\}_{k=1}^{\infty}$ forms a complete orthonormal basis of $L^2(\Omega)$, we have

$$g^p(x) = \frac{\varphi_p(x)}{\sqrt{\lambda_p}\, E_{\alpha,1}(-\lambda_p T^\alpha)}.$$

On the other hand, let us choose other input final data as $h_2 \equiv 0$. By Proposition 3.3, the initial value corresponding to h_0 is $g \equiv 0$. An error in L^2 norm between two input final data is

$$\|h_p - h_0\|_{L^2(\Omega)} = \left\| \frac{\varphi_p}{\sqrt{\lambda_p}} \right\|_{L^2(\Omega)}.$$

Since the family $\{\varphi_k\}_{k=1}^{\infty}$ forms an orthonormal basis of $L^2(\Omega)$, one can get

$$\|h_p - h_0\|_{L^2(\Omega)} = \frac{1}{\sqrt{\lambda_p}}.$$

It follows

$$\lim_{p\to\infty} \|h_p - h_0\|_{L^2(\Omega)} = 0. \tag{12}$$

The error in the L^2 norm between the two corresponding initial values is

$$\|g^p - g\|_{L^2(\Omega)} = \left\| \frac{\varphi_p}{\sqrt{\lambda_p}\, E_{\alpha,1}(-\lambda_p T^\alpha)} \right\|_{L^2(\Omega)} = \frac{1}{\sqrt{\lambda_p}\, E_{\alpha,1}(-\lambda_p T^\alpha)}.$$

From Lemma 2.4, we deduce that there exists $C = C(T, \alpha, C_0) > 0$ such that

$$\|g^p - g\|_{L^2(\Omega)} \geq C \sqrt{\lambda_p}\,.$$

This leads to

$$\lim_{p\to\infty} \|g^p - g\|_{L^2(\Omega)} = +\infty. \tag{13}$$

Combining (12) and (13), we conclude that the inverse problem that we consider is ill-posed.

In order to handle the possible numerical instability of the inverse problem, there are some regularization methods in the literature. For instance, the quasi-reversibility method [33], an alternate iterative method [32], and the quasi-boundary value method [2]. In the current work, we employ one of the most commonly used methods for the regularization of ill-posed problems, that is, the Tikhonov regularization method. We define the Tikhonov regularization functional as follows:

$$\mathcal{T}_\nu(g) := \frac{1}{2}\left\|\mathcal{A}(g) - h^\theta\right\|^2_{L^2(\Omega)} + \frac{\gamma}{2}\left\|g\right\|^2_{L^2(\Omega)},$$

where $\gamma > 0$ is a positive constant, called the regularization parameter. In the function above, the first term denotes the defect between the exact data and the noisy data, and the second term is a penalty term for stabilizing the numerical solution. Consequently, the considered inverse problem may be reformulated and modeled by the following regularized optimization problem:

$$(\mathcal{P}_{op}) \begin{cases} \text{Find } g^\star \in L^2(\Omega) \text{ such that} \\ \\ \mathcal{T}_\nu(g^\star) := \min\limits_{g\in L^2(\Omega)} \mathcal{T}_\nu(g). \end{cases}$$

We know that for problem $(\mathcal{P}_{op})$, there exists a unique minimizer g^θ_γ called Tikhonov regularized solution which converges to the exact solution $g^\star$ under a suitable choice of the regularization parameter γ, see [17]. For more details about the analysis of the optimization problem, interested readers can follow the same technique developed in [1, 8, 9, 26, 27]. The next section is concerned with a numerical method for finding the unique minimizer of the Tikhonov regularization functional $\mathcal{T}_\nu(g)$.

4. Reconstruction approach

This section is devoted to numerical reconstruction approach for solving the minimization problem $(\mathcal{P}_{op})$. The proposed approach is based on two steps:

- The first one is concerned with the derivation of an optimality condition that provides a new characterization of the unknown term $g^\star$.
- The second one is that we employ the conjugate gradient algorithm to solve the variational problem.

Now we derive a first-order optimality condition that provides a simplified characterization of the unknown initial value $g^\star$. The determination of this condition is based on the calculation of the gradient of $\mathcal{T}_\nu$, which can be obtained by constructing an adjoint problem.

Hereafter, we denote by u_g the solution of (1) to emphasize its dependency upon the unknown function g. We point out that the weak formulation of problem (1) reads as follows: Find $u_g \in \mathcal{H}^{\alpha,s}(0, T; \Omega)$ such that $u_g(., 0) = 0$ and

$$\int_0^T \int_\Omega \partial_t^\alpha u_g\, w\, dx\, dt + \int_0^T \mathcal{B}_s(u_g(., t), w(., t))\, dt = 0, \tag{14}$$

for any test function $w \in H^\alpha(0, T; \widetilde{H}^s(\Omega) \cap H^{s+\gamma}(\Omega))$ with $J_{T^-}^{1-\alpha} w = 0$ in $\Omega \times \{T\}$.

Remark 4.1. *The map $g \longmapsto u_g$ is differentiable in the sense of Fréchet and the linearity of* (1) *immediately yields*

$$u_g' \cdot p = \lim_{\epsilon \to 0} \frac{u_{g+\epsilon p} - u_g}{\epsilon} = u_p, \quad \forall p \in L^2(\Omega),$$

here $u_g' \cdot p$ denotes the Fréchet derivative of u_g in the direction p and u_p is the solution problem of (1) *with $g = p$. Notice that, from Proposition 2.2 and the identity* (14)*, one can check that the function u_p satisfies*

$$\int_0^T \int_\Omega u_p \, D_t^\alpha w \, dx \, dt + \int_0^T \mathcal{B}_s(u_p(.,t), w(.,t)) \, dt = \int_\Omega p(x) \, J_{T^-}^{1-\alpha} w(x,0) \, dx, \tag{15}$$

for any test function $w \in H^\alpha(0,T;\widetilde{H}^s(\Omega) \cap H^{s+\gamma}(\Omega))$ with $J_{T^-}^{1-\alpha} w = 0$ in $\Omega \times \{T\}$.

In order to establish the optimality condition, we need the Fréchet derivative $\mathcal{T}_\nu'(g)$ of the objective functional $\mathcal{T}_\nu(g)$. By simple calculations, one can easily derive the following:

$$\begin{aligned} \mathcal{T}_\nu'(g) \cdot p &= \lim_{\epsilon \to 0} \frac{\mathcal{T}_\nu(g+\epsilon p) - \mathcal{T}_\nu(g)}{\epsilon} \\ &= \int_\Omega \left[u_g(x,T) - h^\theta(x) \right] u_p(x,T) \, dx + \gamma \int_\Omega g(x) \, p(x) \, dx. \end{aligned} \tag{16}$$

In order to reduce the computational costs for the Fréchet derivatives, we state it in the natural form. Namely, we need to find an explicit function $R(x)$ such that $\mathcal{T}_\nu'(g) \cdot p = (R, p)$. So, we need to replace the term $\int_\Omega \left[u_g(x,T) - h^\theta(x) \right] u_p(x,T) \, dx$ in (16) by p times a function of x. Therefore, we introduce the following adjoint problem:

$$\begin{cases} \partial_{T^-}^\alpha z_g = -(-\Delta)^s z_g + (u_g(.,T) - h^\theta) \, \delta(t-T), & (x,t) \in \Omega \times (0,T], \\ z_g = 0, & (x,t) \in \Omega^c \times (0,T], \\ z_g = 0, & (x,t) \in \Omega \times \{T\}, \end{cases} \tag{17}$$

where $\delta(t-T)$ is the Dirac delta function at the time $t = T$. The weak formulation of the adjoint problem (17) reads as: Find $z_g \in H^\alpha(0,T;\widetilde{H}^s(\Omega) \cap H^{s+\gamma}(\Omega))$ such that $J_{T^-}^{1-\alpha} z_g = 0$ in $\Omega \times \{T\}$ and

$$\int_0^T \int_\Omega D_t^\alpha z_g \, w \, dx \, dt + \int_0^T \mathcal{B}_s(z_g(.,t), w(.,t)) \, dt = \int_\Omega (u_g(x,T) - h^\theta) \, w(x,T) \, dx, \tag{18}$$

for any test function $w \in W^{\alpha,s}(0,T;\Omega)$ with $w(.0) = 0$ in Ω. After these considerations, we can take z_g and u_p as mutual test functions in identities (15) and (18) and we get

$$\int_\Omega \left[u_g(x,T) - h^\theta(x) \right] u_p(x,T) \, dx := \int_\Omega p(x) \, J_{T^-}^{1-\alpha} z_g(x,0) \, dx. \tag{19}$$

Therefore (19) in (16) yields

$$\mathcal{T}_\nu'(g) \cdot p = \int_\Omega J_{T^-}^{1-\alpha} z_g(x,0) \, p(x) \, dx + \gamma \int_\Omega g(x) \, p(x) \, dx.$$

Based on the above identity, we deduce that the solution to the minimization problem $(\mathcal{P}_{op})$ satisfies the following optimality condition

$$J_{T^-}^{1-\alpha} z_{g^\star}(.,0) + \gamma g^\star = 0, \quad \text{in } \Omega.$$

Next we propose a numerical algorithm for identifying the minimizer of function $\mathcal{T}_\nu(g)$ from noisy measurement of the final time. The numerical algorithm that we propose is based on the conjugate gradient method and Morozov's discrepancy principle (see, e.g., [41]). Let g_k be the kth approximate solution to $g(x)$. Denote

$$g_{k+1} = g_k + \zeta_k \, d_k, \quad k = 0, 1, 2, \cdots, \tag{20}$$

where the initial guess g_0 is given, the term ζ_k is the step size, and d_k is a descent direction in the kth iteration. The conjugate gradient method uses the following iteration formula to update the descent direction:

$$d_k = \begin{cases} -\mathcal{T}_\nu'(g_0) & \text{if} \quad k = 0, \\ -\mathcal{T}_\nu'(g_k) + \alpha_k\, d_{k-1} & \text{if} \quad k \geq 1, \end{cases} \tag{21}$$

where α_k is the conjugate coefficient and calculated as follows:

$$\alpha_k = \begin{cases} 0 & \text{if} \quad k = 0, \\ \dfrac{\int_\Omega \left|\mathcal{T}_\nu'(g_k)\right|^2 \mathrm{d}x}{\int_\Omega \left|\mathcal{T}_\nu'(g_{k-1})\right|^2 \mathrm{d}x} & \text{if} \quad k \geq 1. \end{cases} \tag{22}$$

Since the problem (1) is linear with respect to the initial value g, one can deduce from (16) that

$$\mathcal{T}_\nu(g_k + \zeta_k\, d_k) = \frac{1}{2}\int_\Omega \left(u_{g_k}(x,T) + \zeta_k\, u_{d_k}(x,T) - h^\theta(x)\right)^2 dx + \frac{\gamma}{2}\int_\Omega \left(g_k + \zeta_k\, d_k\right)^2 dx.$$

To this end, we determine the step size ζ_k by imposing the following condition

$$\frac{\partial \mathcal{T}_\nu}{\partial \zeta}(g_k + \zeta_k d_k) = 0.$$

Therefore,

$$\zeta_k = -\frac{\int_\Omega \left(u_{g_k}(x,T) - h^\theta\right) u_{d_k}(x,T)\, dx + \gamma \int_\Omega g_k\, d_k\, dx}{\int_\Omega u_{d_k}^2(x,T)\, dx + \gamma \int_\Omega d_k^2\, dx}. \tag{23}$$

We can summarize the main steps of our reconstruction approach in the following algorithm:

Algorithm 2 *Conjugate Gradient Method* **(CGM)**

1. Initialize g_0 and set $k = 0$.
2. Solve the direct problem (1) with $g = g_k$, and compute the residual:

$$r_k = u_{g_k}(x,T) - h^\theta(x), \quad x \in \Omega.$$

3. Solve the adjoint problem (17) and evaluate the gradient $\mathcal{T}_\nu'(g_k)$.
4. Compute the conjugate coefficient α_k using (22), and determine the search direction d_k via (21).
5. Solve the direct problem (1) with $g = d_k$ to obtain u_{d_k}.
6. Compute the step size ζ_k using (23).
7. Update the initial value using:

$$g_{k+1} = g_k + \zeta_k d_k,$$

as defined in (20).

8. Set $k \leftarrow k + 1$, and return to Step (2). Repeat the procedure until a stopping criterion is met.

Notice that the most important point is to find a suitable stopping rule for an iteration procedure. To deal with this issue, we use the well-known Morozov's discrepancy principle [42]. It is shown that

$$\mathcal{R}_k \leqslant \sigma\theta < \mathcal{R}_{k-1}, \quad \text{with} \quad \mathcal{R}_k = \|r_k\|_{L^2(\Omega)} \quad \text{for each} \quad k \in \mathbb{N}, \tag{24}$$

is sufficient for convergence. It means that we choose the stopping index $\mathcal{I}_s$ such that the inequality (24) is fulfilled, see Hanke and Hansen [25]. Otherwise, if the given input data h^θ is exact (without noise, i.e. $\theta = 0$), we set the stopping index is $\mathcal{I}_s = 100$. The convergence of the proposed method is addressed in [20, 55] and it has been successfully employed for solving some inverse problems, for instance, see [26, 48, 52, 53].

5. Numerical Experiments

In this section, we present the numerical implementation of the proposed reconstruction approach along with corresponding numerical results. Specifically, we apply the iterative algorithm **(CGM)** developed in the previous section to solve problem ($\mathcal{P}_{op}$), which concerns the identification of the initial value g in the initial-boundary value problem (1).

The parameters and their respective values used in the numerical simulations are listed below:

- The spatial domain is chosen as $\Omega = (-1, 1)$.
- The final time is set to $T = 1$.
- The constant σ in (24) is set to $\sigma = 1.01$.
- In the adjoint problem (17), the Dirac delta function is approximated by

$$\delta(t - T) \approx \frac{e^{-(t-T)^2/\eta^2}}{\eta\sqrt{\pi}},$$

  where $\eta > 0$ is a small parameter. We take $\eta = 10^{-3}$.
- The initial guess g_0 is taken to be a constant function, for instance, $g_0 \equiv 1$.

With the exact solution g_{ex}, we produce the noisy final data h^θ by adding a random perturbation, i.e.

$$h^\theta(x) := h(x) + \mu\, h(x)\Big[2\, rand(\text{size}(h)) - 1\Big], \quad x \in \overline{\Omega}.$$

Here $\mu \geq 0$ and $rand(.)$ denote the relative noise level and the uniformly distributed random number in $(0, 1)$, respectively. The function h represents the solution at the final time to the problem (1) with initial value $g = g_{ex}$, that is $h(x) = u_{g_{ex}}(x, T)$, $x \in \overline{\Omega}$. The corresponding noise level is calculated by

$$\theta = \|h^\theta - h\|_{L^2(\Omega)}.$$

In order to evaluate the performance of the conjugate gradient algorithm **(CGM)**, we introduce a L^2-error function E_k defined as

$$E_k = \|g_{ex} - g_k\|_{L^2(\Omega)},$$

which is the error between the exact solution g_{ex} and the reconstructed one g_k at the kth iteration.

In order to apply the proposed algorithm, we need to solve the forward problem (1) and the adjoint problem (17) numerically. Since it is very difficult to know the eigenpairs $\{(\varphi_k, \lambda_k)\}_{k=1}^{\infty}$ associated to the operator $(-\Delta)^s$ in the explicit forms. Thus, in this study, we use an approximation method, similar to the one in [8] to solve the direct and adjoint problems in each iteration instead of using (4), and the series solution of the adjoint problem. Namely, we use a fully discrete approximation based on:

- *A finite difference scheme:* This method is introduced by Y. Liu et al [36] to discretize the Caputo derivative in time. It is proved that this method is of order $2 - \alpha$.
- *The standard* $\mathbb{P}_1$ *finite element method:* This one is utilized for the space approximation. The authors in [3, 10] utilized this method to find an approximate solution to the following elliptic problem involving the fractional Laplace operator:

$$\begin{cases} (-\Delta)^s u = f & \text{in } \Omega, \\ u = 0 & \text{in } \Omega^c. \end{cases}$$

They proved that the convergence order of this method depends on the regularity of the right-hand side f, that is

$$\eth(s) := \begin{cases} \frac{1}{2} + \beta & \text{if} \quad f \in H^{\frac{1}{2}-s}(\Omega), \\ 2\beta & \text{if} \quad f \in L^2(\Omega), \end{cases}$$

where $\beta = \min\{s, \frac{1}{2}\}$.

In order to illustrate the performance of the proposed numerical approach, we solve the direct problem numerically. Namely, we find the approximate solution to the following problem:

$$\begin{cases} \partial_t^\alpha u = -(-\Delta)^s u + F, & (x,t) \in \Omega \times (0,T), \\ u = 0, & (x,t) \in \Omega^c \times (0,T), \\ u = g, & (x,t) \in \Omega \times \{0\}. \end{cases}$$

By choosing

$$F(x,t) = 1 + t^\alpha + \frac{\Gamma(1+\alpha)\ \sqrt{\pi}\, 2^{-2s} \left(1-x^2\right)^s}{\Gamma(s+1/2)\,\Gamma(s+1)} \text{ and } g(x) = \frac{\sqrt{\pi}\, 2^{-2s} \left(1-x^2\right)^s}{\Gamma(s+1/2)\,\Gamma(s+1)},$$

then the unique solution to the above problem reads as

$$u_{ex}(x,t) = (1+t^\alpha)\, \frac{\sqrt{\pi}\, 2^{-2s} \left(1-x^2\right)^s}{\Gamma(s+1/2)\,\Gamma(s+1)}\, \chi_{(-1,1)}(x),\ \forall (x,t) \in (-1,1) \times (0,T),$$

where $\chi_{(-1,1)}$ denotes the characteristic function of the interval $(-1,1)$.

In our computation, we divide the interval Ω into N equally spaced subintervals, with a mesh size $\Delta x = 1/N$. Similarly, the time interval $[0,T]$ will be divided uniformly into K subintervals, and by $\Delta t = 1/K$ we denote the time step. In order to illustrate the accuracy of the proposed approximation method, we measure the L^2-error $\|u_{ex} - u_{app}\|_{L^2(\Omega)}$ evaluated at the final time T. In the following, we examine the time and spatial convergence. A fixed small time step ($\Delta t = 1/200$) is taken to see the spatial convergence and vice-versa. In Table 1, we show the temporal and spatial convergence rates, indicated in the column rate (the number in the bracket is the theoretical rate), for different values of α and s, which fully confirm the theoretical results obtained in [36] for the time discretization and in [3, 10] for the spatial one.

Derivative orders \ Step size		1/50	1/100	1/200	1/400	**rate**
$s = 0.5$	$\alpha = 0.3$	$3.66e-04$	$1.11e-04$	$3.37e-05$	$1.07e-05$	1.69 **(1.7)**
	$\alpha = 0.8$	$2.74e-04$	$1.20e-04$	$4.93e-05$	$2.25e-05$	1.21 **(1.2)**
$\alpha = 0.5$	$s = 0.2$	$9.35e-03$	$6.03e-03$	$3.84e-03$	$2.43e-03$	0.64 **(0.7)**
	$s = 0.9$	$2.92e-04$	$1.59e-04$	$8.36e-05$	$4.30e-05$	0.92 **(1)**

Table 1: Values of the L^2-error function relative to the step size variation.

In Figure 1, we plot the errors in the L^2-norm as a function of the (time or space) step sizes. A logarithmic scale has been used for both step-axis and error-axis in these figures.

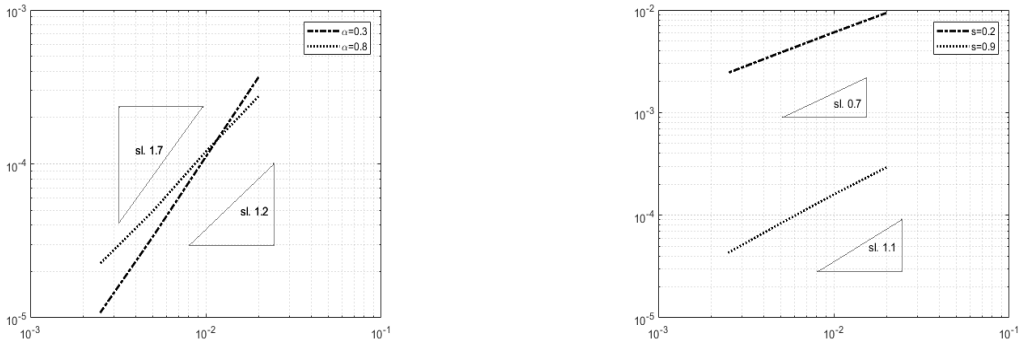

(a) with respect to Δt (b) with respect to Δx

Figure 1: Evolution of the L^2- error functions with respect to the step sizes (sl: slope).

From Table 1 and Figure 1, one can observe that the numerical results show $O(\Delta t^{2-\alpha})$ and $O(\Delta x^{\eth(s)})$ convergence rates in the $L2-$norm for the temporal and spatial discretization, respectively. Therefore, one can conclude that the numerical and theoretical convergence rates (obtained in [3, 10, 36]) are nearly identical. To this end, we plot in Figure 2 the variations of the exact u_{ex} and the approximate solutions u_{app} at time $t = 0.5$ for different values of the derivatives orders α and s for showing the quality of the obtained results.

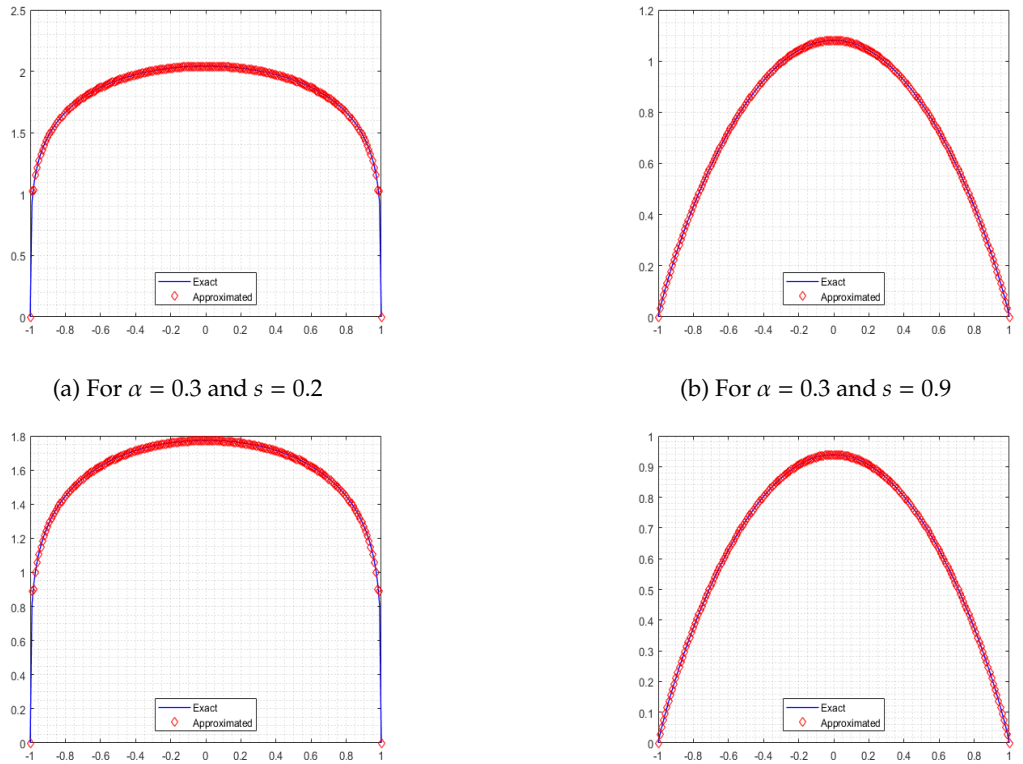

(a) For $\alpha = 0.3$ and $s = 0.2$ (b) For $\alpha = 0.3$ and $s = 0.9$

(c) For $\alpha = 0.8$ and $s = 0.2$ (d) For $\alpha = 0.8$ and $s = 0.9$

Figure 2: Exact and approximate solutions for different values of the fractional derivatives orders α and s.

In the rest of the paper, the grid size for the time and space variables will be taken to be $\Delta t = \Delta x = \frac{1}{100}$.

Then we test the performance of the proposed procedure in finding an estimate of the solution of the minimization problem $(\mathcal{P}_{op})$. More precisely, we will discuss the influence of some parameters such as the fractional derivatives orders α and s, the regularization parameter γ, the smoothness of the function to be reconstructed, and the level of noise θ.

Example 5.1. In this example, we study the influence of the fractional derivatives orders α and s on the quality of the reconstructed results. In doing so, we apply the iterative procedure **(CGM)** to recover

$$g_{ex}(x) = \cos(\pi x)\,\sin(\pi x),$$

with $(\alpha, s) \in \{0.3, 0.8\} \times \{0.2, 0.9\}$ from an exact final data (i.e., from h^{θ}, with $\mu = 0$). The results of this test example are illustrated in Figure 3.

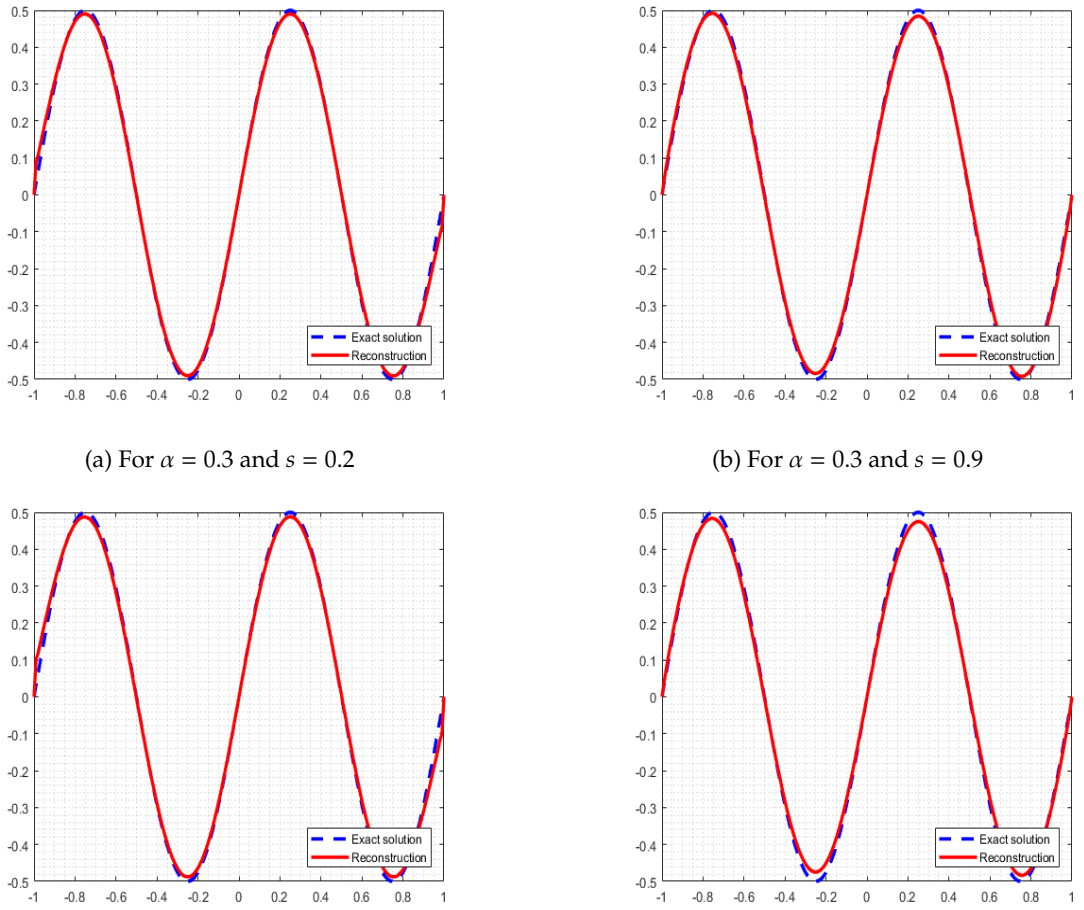

(a) For $\alpha = 0.3$ and $s = 0.2$

(b) For $\alpha = 0.3$ and $s = 0.9$

(c) For $\alpha = 0.8$ and $s = 0.2$

(d) For $\alpha = 0.8$ and $s = 0.9$

Figure 3: Exact (blue dashed line) and Reconstructed functions (red line).

The choices of α and s in this test and the corresponding numerical performances are listed in Table 2.

(α, s)	$(0.3, 0.2)$	$(0.3, 0.9)$	$(0.8, 0.2)$	$(0.8, 0.9)$
E_k	0.00654	0.00811	0.00783	0.00827

Table 2: Choices of the fractional derivatives orders α and s along with the errors E_k.

From Figure 3 and Table 2, one can conclude that the numerical results are quite accurate to the exact solution for each choice of the pairs (α, s). It means that the parameters α and s have no significant influence on the reconstruction results. Therefore, based on the above remarks, the fractional derivatives orders α and s will be fixed to be $(\alpha, s) = (0.5, 0.5)$ in the examples below.

Example 5.2. As it is shown in Section 3, the considered inverse problem is ill-posed in the Hadamard sense and a regularization principle is a key tool to find a stable solution. But choosing an appropriate (not the optimal) value for the regularization parameter γ is a crucial issue. In this study, we use the Tikhonov regularization which is a typical example of an a-priori parameter choice rule since the choice of $\gamma > 0$ is made a-priori (depends only on the noise level $\theta > 0$). Referring to [19, 41], the regularization parameter γ can be chosen such that the consistency condition

$$\lim_{\gamma \to 0} \frac{\theta}{\sqrt{\gamma}} = 0$$

is satisfied. Thus, the parameter γ can be taken to be $\gamma = 10^{-2} \times \theta^{4/5}$. In order to present the importance of the regularization technique for stabilizing our inverse problem, we apply our iterative procedure to reconstruct the initial value g_{ex} for $\gamma = 0$ and $\gamma = 10^{-2} \times \theta^{4/5}$ by taking a stopping index $\mathcal{I}_s = 100$. For this purpose, we test our algorithm in the two following cases:

(i) **Slightly noisy data:** In this case, we assume that the measured final data h^θ is perturbed by low relative noise levels. In Figure 4, we compare the recovered solutions with the exact one in the cases of $\gamma = 0$ and $\gamma = 10^{-2} \times \theta^{4/5}$ with $\mu \in \{0.001, 0.005, 0.01\}$.

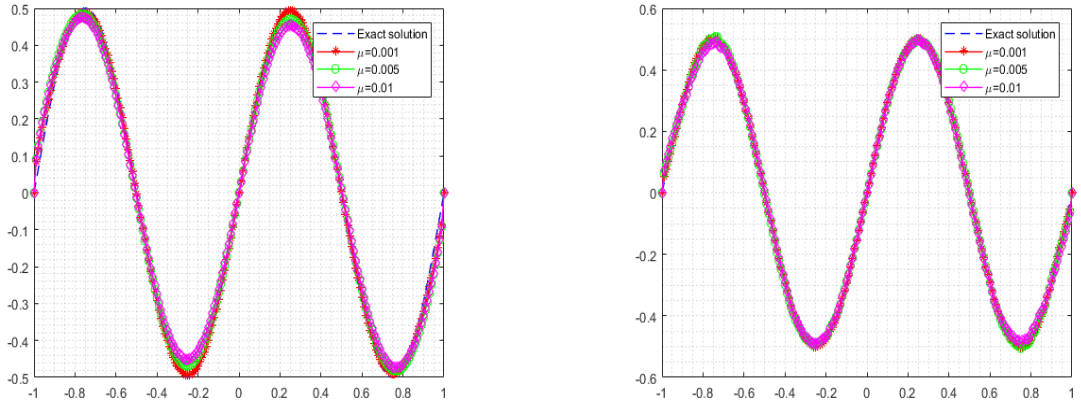

(a) With $\gamma = 0$ (b) With $\gamma = 10^{-2} \times \theta^{4/5}$

Figure 4: Exact solution g_{ex} and their reconstructions g_k obtained by **(CGM)** with $\mu \in \{0.001, 0.005, 0.01\}$. Left: with $\gamma = 0$; Right: with $\gamma = 10^{-2} \times \theta^{4/5}$.

As one can observe from Figure 4 that the numerical approximations of g_{ex} without using the regularization (see Figure 4a) are almost similar to those obtained when $\gamma = 10^{-2} \times \theta^{4/5}$ (see Figure 4b).

(*ii*) **Highly noisy data:** In this case, we consider the case where the measured data is perturbed by a high-levels of noise. We illustrate the comparisons of recovered solutions with the exact one, in Figure 5, but now with $\mu \geq 0.05$, more precisely with relative levels noise $\mu \in \{0.05, 0.1, 0.15\}$.

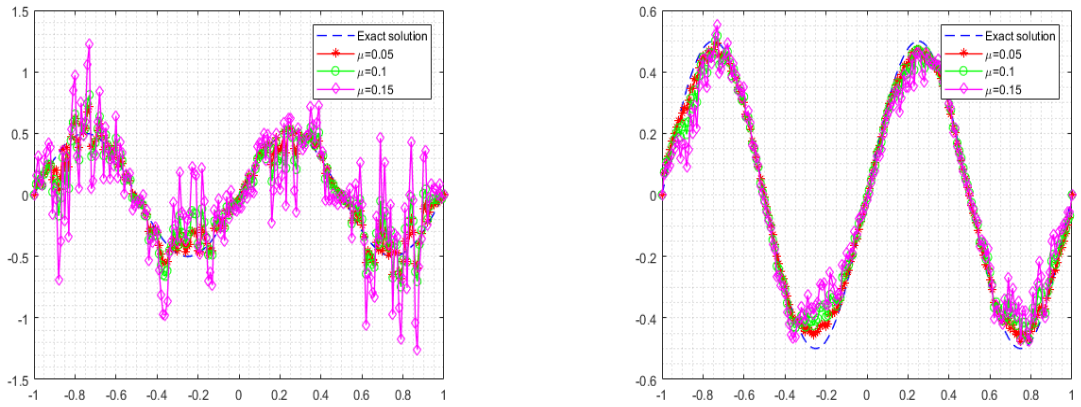

(a) With $\gamma = 0$ (b) With $\gamma = 10^{-2} \times \theta^{4/5}$

Figure 5: Exact solution g_{ex} and their reconstructions g_k obtained by **(CGM)** with $\mu \in \{0.05, 0.1, 0.15\}$. Left: with $\gamma = 0$; Right: with $\gamma = 10^{-2} \times \theta^{4/5}$.

From Figure 5a, one can conclude that the numerical approximations of g_{ex}, without using the regularization (i.e. $\gamma = 0$), have somewhat amplitude of oscillations and they are very unstable and far away from the exact one. However, by using the regularization technique (i.e. $\gamma = 10^{-2} \times \theta^{4/5}$), it can be clearly seen in Figure 5b that the amplitude of the oscillations decreases and numerical results become more accurate.

We also conclude the following from example 5.2:

- If the measured data is slightly perturbed, the proposed algorithm **(CGM)** provides stable numerical solutions to the minimization problem $(\mathcal{P}_{op})$ without the need to use the Tikhonov regularization term (i.e. $\gamma = 0$).

- If the final measured data h^θ is perturbed by high levels of noise, the proposed regularization method is necessary to solve the ill-posed inverse problem.

This behavior is characteristic of ill-posed problems. Thus, in the examples below, the regularization parameter γ will be taken to be $\gamma = 10^{-2} \times \theta^{4/5}$.

In the following examples, we test the performance of the proposed algorithm to reconstruct two examples of initial values (smooth and nonsmooth functions) by combining the conjugate gradient method with Morozov's discrepancy principle. For each example, we investigate the convergence of the proposed approach and present the reconstruction results for various choices of the parameter μ.

Example 5.3. In this example,we test the numerical performance of algorithm **(CGM)** in recovering a smooth initial value given by

$$g_{ex}^{sm}(x) = \sin(\pi x)\, e^{-x^2} - cos(\pi x)\, e^{x^2},$$

with various choices of the relative noise level μ (see Table 3). First, we investigate the convergence of the proposed algorithm and indicate the stopping index $\mathcal{I}_s$ which is determined as

$$\mathcal{I}_s = \begin{cases} 100 & \text{if} \quad \mu = 0, \\ \inf \mathcal{E}_\theta & \text{if} \quad \mu > 0, \end{cases}$$

where the set $\mathcal{E}_\theta$ is given by $\mathcal{E}_\theta := \left\{k \text{ such that } \mathcal{R}_k \leqslant \sigma\theta < \mathcal{R}_{k-1}\right\}$. Figure 6a shows the convergence of the identification process corresponding to each considered noise level for iteration steps $k = 1 : 100$. To determine the stopping index $\mathcal{I}_s$ for each considered noise level, we illustrate the variations of the residuals $\mathcal{R}_k$ in Figure 6b.

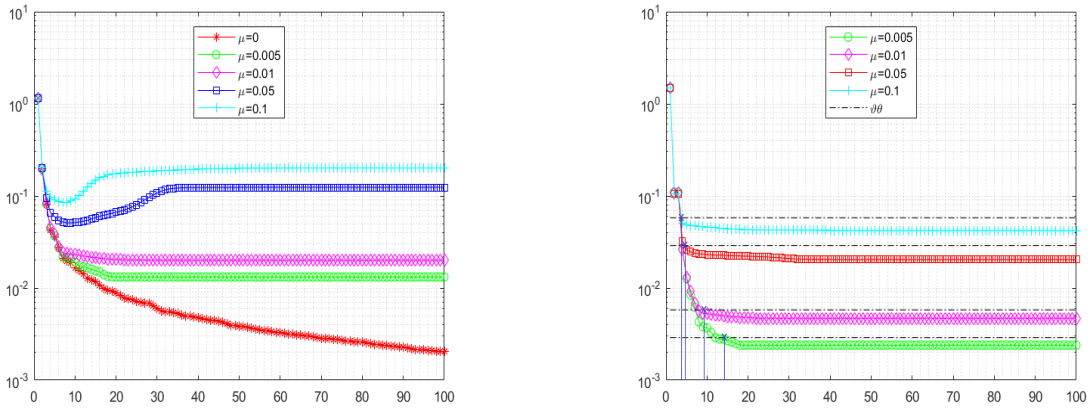

(a) The errors E_k

(b) The residuals $\mathcal{R}_k$

Figure 6: The errors E_k and the residuals $\mathcal{R}_k$ associated to the reconstruction of g_{ex}^{sm} for various relative noise levels (x: stopping index).

μ	0.005	0.01	0.05	0.1
$\mathcal{I}_s$	14	9	5	4

Table 3: The obtained stopping indices $\mathcal{I}_s$ associated to the reconstruction of g_{ex}^{sm}.

According to the stopping indices listed in Table 3, we illustrate the numerical results by using the discrepancy principle in Figure 7.

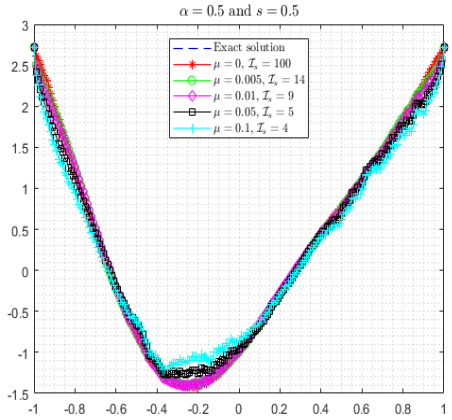

Figure 7: The numerical results of g_{ex}^{sm} for various relative noise levels.

Example 5.4. In this example, we reconstruct a nonsmooth initial value given by

$$g_{ex}^{nsm}(x) = \begin{cases} 0.5, & x \in [-1, -0.75) \cup (0.75, 1], \\ 1, & x \in [-0.75, -0.25) \cup (0.25, 0.75], \\ 2, & x \in [-0.25, 0.25], \end{cases}$$

with the same relative noise levels chosen in Example 5.3. We present the convergence of the estimated solutions to the exact one in Figure 8. More precisely, we illustrate the approximation errors E_k and residuals $\mathcal{R}_k$ for iteration steps $k = 1 : 100$ with the considered choices of the parameters μ in Figures 8a and 8b, respectively.

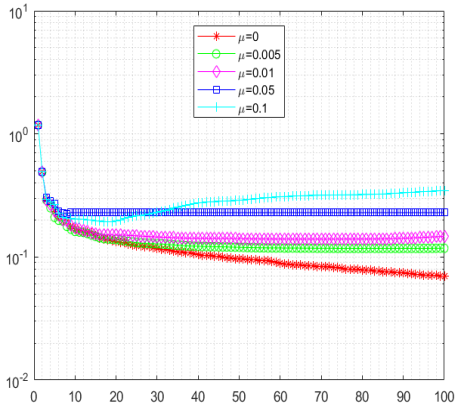

(a) The errors E_k

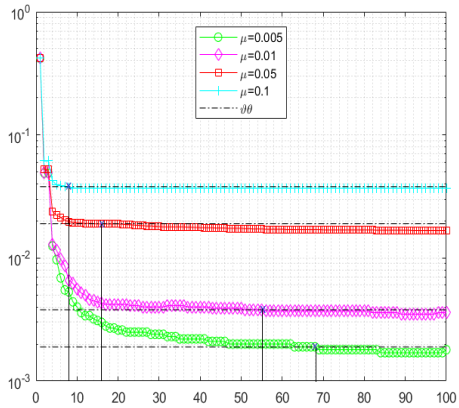

(b) The residuals $\mathcal{R}_k$

Figure 8: The errors E_k and the residuals $\mathcal{R}_k$ associated to the reconstruction of g_{ex}^{nsm} for various relative noise levels (x: stopping index).

The obtained stopping indices for each choice μ which are determined with the help of curves presented in Figure 8b are listed in Table 4.

μ	0.005	0.01	0.05	0.1
$\mathcal{I}_s$	68	55	16	8

Table 4: The obtained stopping indices $\mathcal{I}_s$ associated to the reconstruction of g_{ex}^{nsm}.

In Figure 9, we illustrate the comparisons of recovered solutions with the exact ones for each considered relative noise level μ.

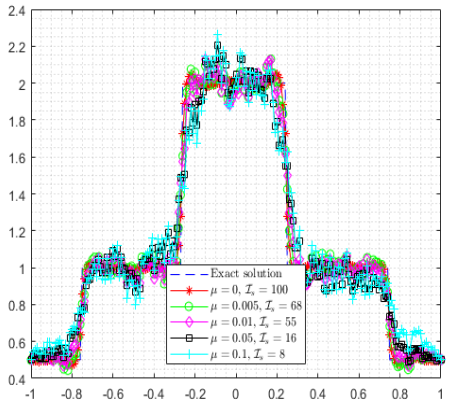

Figure 9: The numerical results of g_{ex}^{nsm} for various relative noise levels.

We draw the following conclusions from Examples 5.3 and 5.4:

- From Figure 9, it can be observed that the presence of singularities significantly affects the accuracy of the reconstructed initial value g_{ex}^{nsm}. Specifically, the performance of our iterative procedure deteriorates markedly in the vicinity of these singular points. In comparison with the results obtained in Example 5.3 (see Figure 7), we conclude that the proposed method performs better when reconstructing smooth functions than in identifying nonsmooth ones.

- As shown in Figures 6a and 8a, the approximation error E_k increases with higher noise levels in the input data h^θ. Furthermore, for a given relative noise level $\mu > 0$, the computed errors tend to plateau or increase slightly after a few iterations. This indicates the necessity of stopping the algorithm at an appropriate iteration. Figures 6b and 8b demonstrate that Morozov's discrepancy principle effectively determines the stopping point by satisfying the condition (24) for each considered noise level $\mu > 0$.

- Figures 7 and 9 indicate that the proposed numerical scheme **(CGM)** is robust against noise and yields reasonably accurate reconstructions. In particular, the numerical results remain reliable with noise levels up to 1% in the final data $u(x, T)$. However, when the relative noise level μ exceeds 0.05, noticeable spurious oscillations begin to appear, degrading the accuracy and quality of the reconstruction. In such cases, the computed solution may deviate significantly from the true solution, highlighting the increased severity of the ill-posedness under high noise conditions. To improve the reconstruction in these scenarios, it is crucial to determine an optimal regularization parameter that adapts to the noise level. Nevertheless, selecting such a parameter is a challenging task, and its theoretical foundation has not yet been fully developed. This remains an open problem and will be addressed in future work.

6. Concluding Remarks

In this work, we investigated an inverse problem associated with a space-time fractional diffusion equation, where the goal is to determine the unknown initial condition from noisy final-time observations. The fractional model accounts for both memory effects and long-range spatial interactions, making it suitable for describing anomalous diffusion processes observed in various physical and biological systems.

We first established the uniqueness of the inverse problem and analyzed its ill-posed nature in the sense of Hadamard. To address the inherent instability, we reformulated the problem as a Tikhonov-regularized optimization problem and derived a first-order optimality condition using an adjoint-based approach. An efficient numerical scheme based on the conjugate gradient method, combined with Morozov's discrepancy principle, was proposed to obtain stable approximate solutions. Through comprehensive numerical experiments, we demonstrated that the method yields accurate reconstructions for both smooth and discontinuous initial data and remains robust under varying levels of measurement noise.

The current study lays the groundwork for several promising avenues of research. Optimal Regularization Parameter Selection: Although a heuristic formula for choosing the Tikhonov regularization parameter was used, a deeper theoretical study on optimal parameter selection (e.g., via a posteriori strategies or bilevel optimization) would enhance solution accuracy and stability. Extension to Multi-dimensional and Irregular Domains: The methodology can be extended to higher-dimensional problems and domains with complex geometries, which are common in real-world applications. Investigating domain discretization techniques such as adaptive finite elements could improve accuracy and computational efficiency. Inverse Problems with Unknown Coefficients: Beyond the initial condition, future work could explore the simultaneous recovery of multiple unknowns—such as fractional orders, source terms, or spatially varying diffusion coefficients—from partial or noisy observations. Time-dependent or Nonlinear Extensions: Incorporating time-dependent or nonlinear diffusion operators (e.g., fractional p-Laplacian or nonlinear memory kernels) would broaden the scope of the current method to model more complex physical systems. Uncertainty Quantification and Bayesian Inference: A probabilistic framework such as Bayesian inversion could be developed to quantify the uncertainty in the reconstructed initial condition and assess the impact of noise or model error on the solution. Data-driven and Learning-based Approaches: Integrating physics-informed neural networks (PINNs) or hybrid data-driven methods with the current regularization framework could lead to new paradigms for solving fractional inverse problems, especially when dealing with limited or scattered data.

We believe that these directions offer rich potential for further advancing the theory and numerical analysis of inverse problems in fractional diffusion models, with broad applications in physics, engineering, biology, and finance.

Acknowledgments

The authors sincerely thank the anonymous referee for their careful reading, for pointing out several errors, and for providing valuable comments and suggestions that have significantly improved the quality of this paper. The authors would also like to express their gratitude to Dr. J. P. Borthagay for his assistance with the computational experiments.

References

[1] M. Abdelwahed, M. BenSaleh, N. Chorfi, M. Hassine, *An inverse problem study related to a fractional diffusion equation*, J. Math. Anal. Appl. **512** (2022), no. 2, 126145.
[2] L. Sh. Abdulkerimov, *Regularization of an ill-posed Cauchy problem for evolution equations in a Banach space*, Azerb. Gos. Univ. Ucen. Zap. Fiz. Mat. **1** (1977), 32–36.
[3] G. Acosta, F. M. Bersetche, and J. P. Borthagaray, A short FE implementation for a 2d homogeneous Dirichlet problem of a fractional Laplacian, *Comput. Math. Appl.* **74** (2017), no. 4, 784–816.

[4] G. Acosta, F. M. Bersetche, J. P. Borthagaray, *Finite element approximations for fractional evolution problems*, Fract. Calc. Appl. Anal. **22** (2019), no. 3, 767–794.
[5] R. A. Adams, *Sobolev spaces*, Academic Press, New York–San Francisco–London, 1975.
[6] O. Agrawal, *Fractional variational calculus in terms of Riesz fractional derivatives*, J. Phys. A: Math. Theor. **40** (2007), no. 24, 6287–6303.
[7] R. Almeida, D. F. M. Torres, *Necessary and sufficient conditions for the fractional calculus of variations with Caputo derivatives*, Commun. Nonlinear Sci. Numer. Simul. **16** (2011), no. 3, 1490–1500.
[8] M. BenSaleh, H. Hassine, *Inverse source problem for a space-time fractional diffusion equation*, Ricerche Mat. (2021), 1–33.
[9] M. BenSalah, M. Hassine, *Inverse source problem for a diffusion equation involving the fractional spectral Laplacian*, Math. Methods Appl. Sci. **44** (2021), no. 1, 917–936.
[10] J. P. Borthagaray, W. Li, and R. H. Nochetto, Fractional elliptic problems on Lipschitz domains: regularity and approximation, *arXiv preprint arXiv:2212.14070*, 2022.
[11] Z.-Q. Chen, M. M. Meerschaert, E. Nane, *Space–time fractional diffusion on bounded domains*, J. Math. Anal. Appl. **393** (2012), no. 2, 479–488.
[12] J. Cheng, J. Nakagawa, M. Yamamoto, T. Yamazaki, *Uniqueness in an inverse problem for a one-dimensional fractional diffusion equation*, Inverse Probl. **25** (2009), no. 11, 115002.
[13] K. Diethelm, *The analysis of fractional differential equations*, Lecture Notes in Mathematics, vol. 2004, Springer-Verlag, Berlin, 2010.
[14] E. Di Nezza, G. Palatucci, E. Valdinoci, *Hitchhiker's guide to the fractional Sobolev spaces*, Bull. Sci. Math. **136** (2012), no. 5, 521–573.
[15] S. Dipierro, X. Ros-Oton, E. Valdinoci, *Nonlocal problems with Neumann boundary conditions*, Rev. Mat. Iberoam. **33** (2017), no. 2, 377–416.
[16] Q. Du, M. Gunzburger, R. B. Lehoucq, K. Zhou, *A nonlocal vector calculus, nonlocal volume-constrained problems, and nonlocal balance laws*, Math. Models Methods Appl. Sci. **23** (2013), no. 3, 493–540.
[17] H. W. Engl, M. Hanke, A. Neubauer, *Regularization of inverse problems*, Springer, Berlin, 1996.
[18] X. Feng, P. Li, X. Wang, *An inverse random source problem for the time-fractional diffusion equation driven by a fractional Brownian motion*, Inverse Probl. **36** (2020), no. 4, 045008.
[19] N. P. Galatsanos and A. K. Katsaggelos, Cross-validation and other criteria for estimating the regularizing parameter, *Proc. ICASSP '91: Int. Conf. Acoustics, Speech, and Signal Processing*, IEEE (1991), 3021–3024.
[20] J. C. Gilbert and J. Nocedal, Global convergence properties of conjugate gradient methods for optimization, *SIAM J. Optim.* **2** (1992), no. 1, 21–42.
[21] R. Gorenflo, F. Mainardi, *Fractional calculus: integral and differential equations of fractional order*, Springer, 1997.
[22] G. Grubb, *Spectral results for mixed problems and fractional elliptic operators*, J. Math. Anal. Appl. **421** (2015), no. 2, 1616–1634.
[23] N. Guerngar, E. Nane, R. Tinaztepe, S. Ulusoy, H. W. Van Wyk, *Simultaneous inversion for the fractional exponents in the space-time fractional diffusion equation*, Fract. Calc. Appl. Anal. **24** (2021), no. 3, 818–847.
[24] J. Hadamard, *Sur les problèmes aux dérivées partielles et leur signification physique*, Princeton Univ. Bull. (1902), 49–52.
[25] M. Hanke and P. C. Hansen, Regularization methods for large-scale problems, *Surv. Math. Ind.* **3** (1993), no. 4, 253–315.
[26] M. Hrizi, M. BenSalah, M. Hassine, *Determination of the initial density in nonlocal diffusion from final time measurements*, Discrete Contin. Dyn. Syst. Ser. S **15** (2022), no. 6.
[27] D. Jiang, Y. Liu, D. Wang, *Numerical reconstruction of the spatial component in the source term of a time-fractional diffusion equation*, Adv. Comput. Math. **46** (2020), 1–24.
[28] B. Jin, W. Rundell, *An inverse problem for a one-dimensional time-fractional diffusion problem*, Inverse Probl. **28** (2012), no. 7, 075010.
[29] E. Karapinar, D. Kumar, R. Sakthivel, N. H. Luc, N. H. Can, *Identifying the space source term problem for time-space-fractional diffusion equation*, Adv. Differ. Equ. **2020** (2020), no. 1, 1–23.
[30] K. H. Karlsen, S. Ulusoy, *Stability of entropy solutions for Lévy mixed hyperbolic-parabolic equations*, arXiv preprint arXiv:0902.0538 (2009).
[31] A. A. Kilbas, H. M. Srivastava, J. J. Trujillo, *Theory and applications of fractional differential equations*, Elsevier, **204**, 2006.
[32] V. A. Kozlov, V. G. Maz'ya, *Iterative procedures for solving ill-posed boundary value problems that preserve the differential equations*, Algebra i Analiz **1** (1989), no. 5, 144–170.
[33] R. Lattès, J.-L. Lions, *The method of quasi-reversibility: applications to partial differential equations*, Tech. Report, 1969.
[34] G. Li, D. Zhang, X. Jia, M. Yamamoto, *Simultaneous inversion for the space-dependent diffusion coefficient and the fractional order in the time-fractional diffusion equation*, Inverse Probl. **29** (2013), no. 6, 065014.
[35] Z. Li, O. Y. Imanuvilov, M. Yamamoto, *Uniqueness in inverse boundary value problems for fractional diffusion equations*, Inverse Probl. **32** (2015), no. 1, 015004.
[36] Y. Lin and C. Xu, Finite difference/spectral approximations for the time-fractional diffusion equation, *J. Comput. Phys.* **225** (2007), no. 2, 1533–1552.
[37] A. Lischke, G. Pang, M. Gulian, F. Song, C. Glusa, X. Zheng, Z. Mao, W. Cai, M. M. Meerschaert, M. Ainsworth, G. E. Karniadakis, *What is the fractional Laplacian? A comparative review with new results*, J. Comput. Phys. **404** (2020), 109009.
[38] J. J. Liu, M. Yamamoto, *A backward problem for the time-fractional diffusion equation*, Appl. Anal. **89** (2010), no. 11, 1769–1788.
[39] Y. Luchko, *Initial-boundary-value problems for the one-dimensional time-fractional diffusion equation*, Fract. Calc. Appl. Anal. **15** (2012), no. 1, 141–160.
[40] M. M. Meerschaert, D. A. Benson, H.-P. Scheffler, B. Baeumer, *Stochastic solution of space-time fractional diffusion equations*, Phys. Rev. E **65** (2002), no. 4, 041103.
[41] V. A. Morozov, Z. Nashed, A. B. Aries, *Methods for Solving Incorrectly Posed Problems*, Springer, New York, 1984.
[42] V. A. Morozov, *Methods for solving incorrectly posed problems*, Springer Science & Business Media, 2012.
[43] H. L. Nguyen, D. Kumar, L. D. Long, H. T. K. Van, *Final value problem for parabolic equation with fractional Laplacian and Kirchhoff's term*, J. Funct. Spaces **2021** (2021), 1–12.
[44] I. Podlubny, *Fractional differential equations*, Mathematics in Science and Engineering, vol. 198, Academic Press, San Diego, 1999.

[45] X. Ros-Oton, J. Serra, *Local integration by parts and Pohozaev identities for higher order fractional Laplacians*, arXiv preprint arXiv:1406.1107 (2014).
[46] K. Sakamoto, M. Yamamoto, *Inverse source problem with a final overdetermination for a fractional diffusion equation*, Math. Control Relat. Fields **1** (2011), no. 4, 509–518.
[47] K. Sakamoto, M. Yamamoto, *Initial value/boundary value problems for fractional diffusion-wave equations and applications to some inverse problems*, J. Math. Anal. Appl. **382** (2011), no. 1, 426–447.
[48] L. Sun and T. Wei, Identification of the zeroth-order coefficient in a time fractional diffusion equation, *Appl. Numer. Math.* **111** (2017), 160–180.
[49] S. Tatar, R. Tınaztepe, S. Ulusoy, *Simultaneous inversion for the exponents of the fractional time and space derivatives in the space-time fractional diffusion equation*, Appl. Anal. **95** (2016), no. 1, 1–23.
[50] S. Tatar, S. Ulusoy, *An inverse source problem for a one-dimensional space–time fractional diffusion equation*, Appl. Anal. **94** (2015), no. 11, 2233–2244.
[51] J.-G. Wang, T. Wei, *Quasi-reversibility method to identify a space-dependent source for the time-fractional diffusion equation*, Appl. Math. Model. **39** (2015), no. 20, 6139–6149.
[52] T. Wei, X.-L. Li, and Y.-S. Li, An inverse time-dependent source problem for a time-fractional diffusion equation, *Inverse Problems* **32** (2016), no. 8, 085003.
[53] X. B. Yan and T. Wei, Inverse space-dependent source problem for a time-fractional diffusion equation by an adjoint problem approach, *J. Inverse Ill-posed Probl.* **27** (2019), no. 1, 1–16.
[54] Y. Zhang, X. Xu, *Inverse source problem for a fractional diffusion equation*, Inverse Probl. **27** (2011), no. 3, 035010.
[55] G.-H. Zheng and T. Wei, Recovering the source and initial value simultaneously in a parabolic equation, *Inverse Problems* **30** (2014), no. 6, 065013.